Preliminary design of a pneumatic drying system

Gowtham Pandiarajan 4738853
Sidharth Krishnan Kalyani 4737237
Sampath Kumar Raghunathan Srikumar 4718879

Faculty of Applied Sciences

TU Delft Delft University of Technology

Faculty of Applied Sciences 10th March, 2019

Contents

List of Symbols

Symbols

A	Cross section Area	m^2
α	Angle of inclination	$^\circ$
ϵ	Void fraction	-
f	Friction factor	-
g	Acceleration due to gravity	m/s^2
ρ	Density	kg/m^3
μ	Dynamic Viscosity	$Pa\ s$
σ	Surface tension of the fluid	N/m
d	Internal diameter	m
r	Radius of the pipe	m
L	Length of the hose	m
ΔP	Pressure differece	Pa
Re	Reynolds Number	
We	Weber number	-
Fr	Froude number	-
v	Velocity	m/s
$\dot{V}$	Volumetric flow	m^3/s
$\dot{M}$	Mass flow rate	kg/s
$\dot{m}$	Mass flux	kg/m^2s
ϕ	Two phase multiplier	-
$\dot{x}$	Gas(air) mass quality	-
S	Surface area	- m^2
s	Velocity slip ratio	-
τ	Wall shear stress	N/m^2

List of Figures

List of Tables

1 Introduction

1.1 Spray drying

A pneumatic powder-dryer can be used for flash evaporation of surface moisture, where heat transfer dominates the drying phenomenon. Pneumatic drying (spray drying) is used in agricultural, food, chemical and pharmaceutical industries. Simply stated, spray drying is a method of producing a dry powder from a liquid or slurry by rapidly drying with a hot gas. But the innate complexity of spray drying involves understanding of the multi-phase flow phenomenon and the proper adaptation and implementation of turbulence models served as the motivation for this project involving the preliminary design of a pneumatic spray drying model. The spray-drying process contains three stages. In the first stage droplets are created by an atomizer, for example a nozzle or a rotary wheel. These droplets then enter the hot airflow and water evaporates from the droplets. Finally, in the last stage the dry particles are separated from the gas flow, at the end of the channel.

1.2 Aim

The main aim of this project is to develop a code which models the turbulence laden multi-phase flow together with a detailed approach into the modeling of drying kinetics of the wet particles. The end goal is to prescribe design recommendations for preliminary design of a spray dryer based on the multiphase flow physics. The objectives in reaching the end goal include implementing k-ϵ model and analysis of dispersed phase.

1.3 Concepts utilized

In order to prescribe the design recommendations, the particle size distribution and drying without particle burnout are the main requirements set. Co-flow is utilized for analysis due to the small size of the particles. One-way coupling is considered , with the usage of Euler-Lagrangian solver. Eulerian method with a Finite-Volume (FV) approach is used for modeling the continuous phase, the dry air. Prandtl mixing length and k-ϵ models are the turbulence models considered. To model the properties of individual particles, Lagrangian approach is utilized for modeling the dispersed phase. A Discrete Random Walk (DRW) model is adapted for this purpose. The drying kinetics of the particles is modelled by considering three drying stages [5][4]. The effect of inlet air velocity, temperature and initial moisture content is utilized to analyze the droplet temperature

and particle size distribution. Based on these analyses, design recommendations for a spray dryer are prescribed.

1.4 Report outline

In the next chapter, the computational setup for continuous phase is explained in detail. Chapter 2 explains the model setup which includes the single phase, the dispersed phase and the drying kinetics of the particles. Results of the above-mentioned analyses are discussed in the following chapter and design recommendations are made based on these analyses.

2 Setup

2.1 Single phase

The computational setup is started by completely configuring the single phase model of the problem. The aim of the single phase setup is to obtain the turbulent flow and temperature field in the entire domain. This is then used to model the dispersed phase.

The domain considered is a 2D channel in which the drying process takes place. The dimensions and the mesh used are shown below. As mentioned in the figure, cosine spacing is used to create the mesh, so that more number of cells are accumulated near the wall.

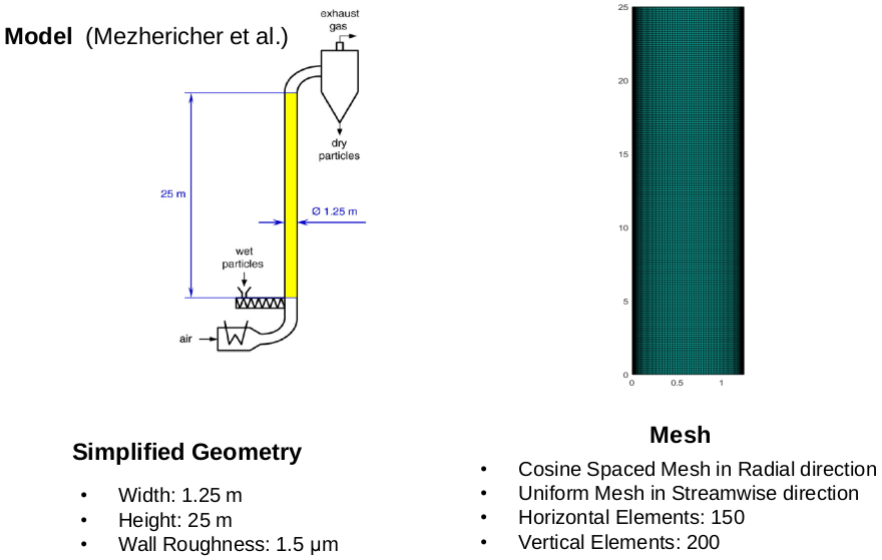

Figure 2.1: Domain dimensions and the mesh used

2.1.1 Flow field

The turbulent flow field is obtained by discretizing and solving the Reynolds Averaged Navier Stokes (RANS) equations. A finite-volume approach is used for discretization. It is assumed that the turbulent flow is fully developed along the length of the channel. Thus the simplified RANS equation applicable for the case is :

$$\frac{\partial(\overline{u'v'})}{\partial y} = -\frac{\partial \overline{p}}{\partial x} + \frac{\partial}{\partial y}\nu\frac{\partial \overline{u}}{\partial y}$$

$$\overline{u'v'} = -\nu_\tau \frac{\partial \overline{u}}{\partial y}$$

The second relation used to approximate the effect of the Reynolds stresses is the eddy-viscosity hypothesis. Closure models are still needed for the eddy viscosity (ν_τ) to close the set of equations. Two models have been used in this report :

2.1.1.1 Prandtl Mixing Length model

This model directly gives an algebraic relation for ν_τ, without the need for any extra transport equations. The model is given as:

$$\nu_\tau = l_m^2 |\frac{\partial \overline{u}}{\partial y}|$$

where l_m is called the mixing length. This is prescribed by the Nikkuradse Polynomial[2].

$$l_m = 0.14R - 0.08R\left(\frac{y}{R}\right)^2 - 0.06R\left(\frac{y}{R}\right)^4$$

where R is the channel half width. One problem with the polynomial is that for y very close to the wall, the mixing length doesn't fall to zero very fast. Therefore, it needs to be damped near the wall to gradually allow it to fall to zero at the wall. For this, Van-Driest damping function for the mixing length is used. This is shown below.

$$l_m = 0.4y\left[1 - e^{\frac{-yRe_\tau}{26R}}\right]$$

To check the accuracy of the Prandtl mixing length model, the obtained velocity field is compared with the DNS data[1] for channel flow at $Re_\tau = 1000$. This is shown below. From the figure, it can be seen that the obtained velocity field is quite accurate.

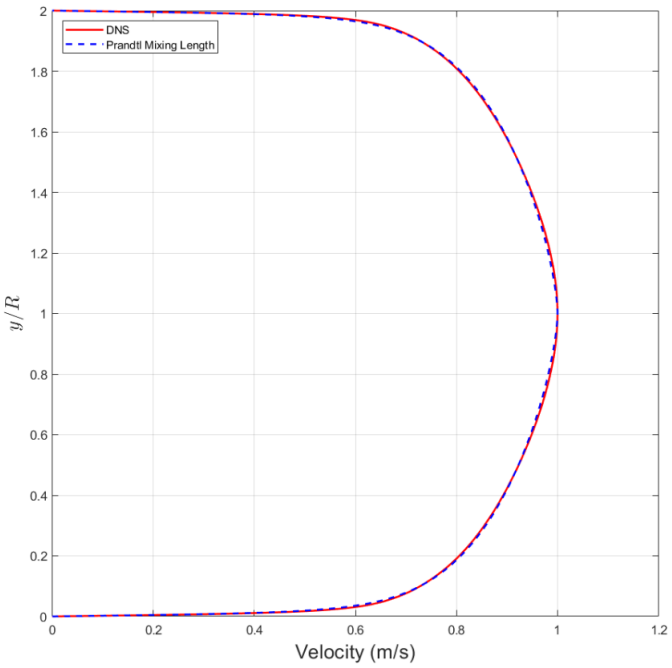

Figure 2.2: Comparison of velocity field from DNS and Prandtl mixing length at $Re_\tau = 1000$

2.1.1.2 K-epsilon model

Even though the mixing length model seems pretty accurate for the channel flow, it doesn't provide any information regarding the kinetic energy (k), that is required for Discrete Random Walk model, discussed subsequently. Therefore, another closure model is required for the eddy-viscosity, and the $k-\epsilon$ model, is considered. This involves utilizing two additional transport equations for the turbulent kinetic energy (k) and the turbulent dissipation rate (ϵ) to solve for the eddy viscosity (μ_τ).

$$-\frac{\partial}{\partial y}\left[\mu + \frac{\mu_\tau}{\sigma_k}\right]\frac{\partial k}{\partial y} = \mu_\tau\left[\frac{\partial u}{\partial y}\right]^2 - \rho\epsilon$$

$$-\frac{\partial}{\partial y}\left[\mu + \frac{\mu_\tau}{\sigma_\epsilon}\right]\frac{\partial \epsilon}{\partial y} = C_{\epsilon_1}\frac{\epsilon\mu_\tau}{k}\left[\frac{\partial u}{\partial y}\right]^2 - C_{\epsilon_2}f_\epsilon\rho\frac{\epsilon^2}{k}$$

$$\mu_\tau = C_\mu f_\mu \frac{k^2}{\epsilon}$$

where σ_k, σ_ϵ, C_{ϵ_1}, C_{ϵ_2}, C_μ are model constants and f_μ, f_ϵ are damping functions for the eddy viscosity. The damping functions prescribed by Myong and Kasagi are used, as they show better agreement with the DNS data[6]. The damping functions are given as:

$$f_\mu = \left[1 - e^{-\left(\frac{y^+}{70}\right)}\right]\left[1 + \frac{3.45}{\sqrt{Re_\tau}}\right]$$

$$f_\epsilon = \left[1 - \frac{2}{9}e^{-\left(\frac{Re_T}{6}\right)^2}\right]\left[1 - e^{-\left(\frac{y^+}{5}\right)}\right]^2$$

To initialize the flow field, the solution obtained from the Prandtl mixing length model is used. This is done to obtain faster convergence. All the spatial discretizations for both k and ϵ are done using first order upwind scheme. Thus the obtained values of k and ϵ are used to calculate the eddy viscosity and subsequently the RANS equations are solved. To check the accuracy of the obtained velocity and turbulent kinetic energy fields, it is compared with the DNS data[1] for a channel flow at $Re_\tau = 1000$.

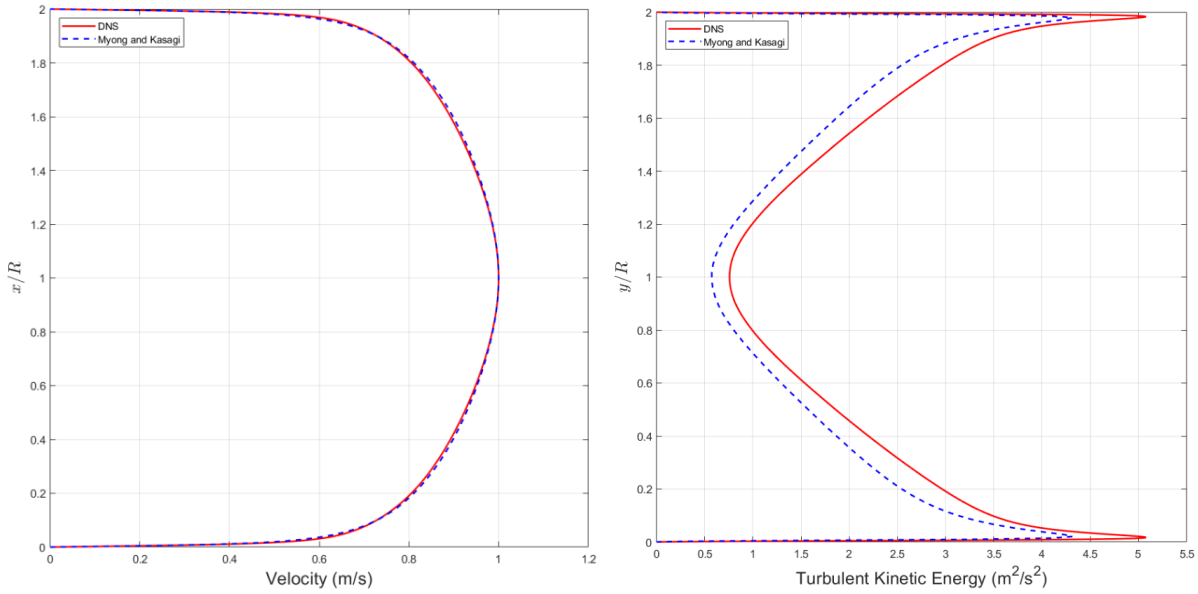

(a) Velocity field

(b) Turbulent kinetic energy

Figure 2.3: Comparison with DNS data at $Re_\tau = 1000$

2.1.2 Temperature field

Once the flow field is obtained from the K-epsilon model, it can be used to get the temperature field in the domain. For that, 2D Reynolds Averaged Temperature (RAT) equation is discretized and solved. The simplified RAT equation is shown below.

$$\overline{u}\frac{\partial \overline{T}}{\partial x} + \frac{\partial(\overline{u'T'})}{\partial x} + \frac{\partial(\overline{v'T'})}{\partial y} = \frac{\partial}{\partial x}\alpha\frac{\partial \overline{T}}{\partial x} + \frac{\partial}{\partial y}\alpha\frac{\partial \overline{T}}{\partial y}$$

As for the flow field, additional equations are required for the terms comprising velocity

and temperature fluctuations. A similar model to the eddy viscosity model, called eddy diffusivity hypothesis is used.

$$\overline{u'T'} = -\alpha_\tau \frac{\partial \overline{T}}{\partial x}$$

$$\overline{v'T'} = -\alpha_\tau \frac{\partial \overline{T}}{\partial y}$$

where α_τ is the turbulent thermal diffusivity. To simplify matters, Reynolds analogy is assumed. According to this assumption, turbulent Prandtl number (Pr_τ) is taken as 1. This is a fair assumption considering that the fluid is air. Therefore,

$$Pr_\tau = 1 \implies \nu_\tau = \alpha_\tau$$

Thus, using these assumptions, the RAT equation can be solved to obtain the temperature field in the entire domain. The converged 2D temperature field contour for a case having the walls at 300 K and dry air entering at 11 m/s with temperature 400 K is shown below.

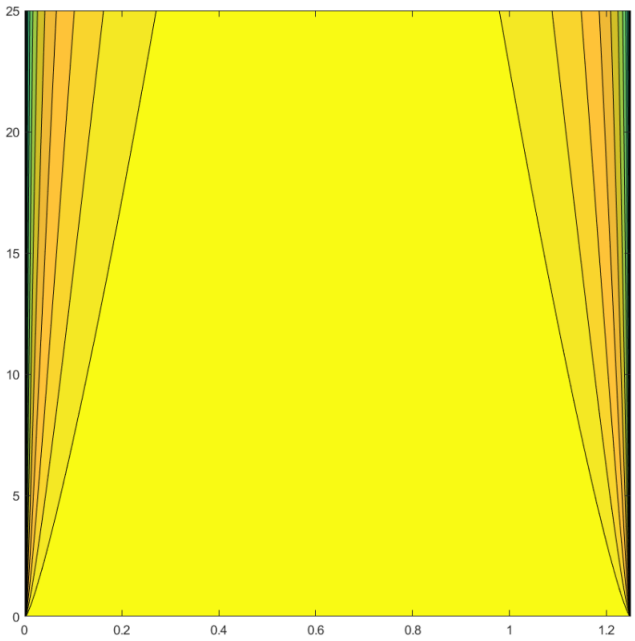

Figure 2.4: 2D temperature contour for a case having the walls at 300 K and dry air entering at 11 m/s with temperature 400 K

Therefore, once the temperature and velocity fields over the domain are obtained, the dispersed phase equations can be solved.

2.2 Dispersed phase

This section deals with equations and the mathematical models required for modelling the forces on the particles. Once the complete velocity and temperature fields of the domain are obtained, they can be used to update the particle positions in each time step. Firstly, the forces acting on a single particle are considered:

- Steady state drag:
$$\overline{F}_D = 3\pi\mu D f(\overline{U} + \overline{U'} - \overline{U}_p)$$

  f - friction factor given by $f = 1 + 0.15Re_r^{0.687}$,a correlation given by Schiller [8] that is reasonably good for a particle Reynolds number up to 800.
  D - Particle diameter,
  μ - Dynamic viscosity of the fluid,
  $\overline{U}$ - Bulk fluid mean velocity,
  $\overline{U'}$ - Fluctuations in the bulk fluid velocity due to turbulence,
  $\overline{U}_p$ - Particle velocity

- Weight of the particle:
$$\overline{F}_W = mg$$

The particle lift forces are assumed to be negligible as the size of the particle is extremely small. Forces such as the virtual mass effect and history forces are not considered since the single phase is assumed as fully developed.

Once the forces are properly defined, the instantaneous particle positions are obtained by using the Newton's second law :

$$m\frac{d\overline{U}_p}{dt} = \overline{F}_D + \overline{F}_W$$
$$\frac{d\overline{x}_p}{dt} = \overline{U}_p$$

These two equations are discretized using Euler implicit scheme and solved.

2.2.1 Discrete Random Walk (DRW) model:

To account for the effects of turbulent fluctuations on the particle position, a stochastic method called Discrete Random Walk (DRW) model[3] is used. Turbulence is generally assumed to be a spectrum of eddies of varying sizes. DRW tries to model the interaction of these eddies with the particle by assuming a particular length scale for the eddy and the interaction time. To do this, the kinetic energy and the dissipation field over the complete domain is used. The definitions of all the parameters required to completely define the DRW model are shown below:

- **Length scale of the eddy (l)**:
  Parameter that defines the eddy size based on kinetic energy and dissipation rate at a position.

$$l = C_\mu \frac{k^{1.5}}{\epsilon}, C_\mu = 0.085$$

- **Eddy lifetime (T_E)**:
  Parameter that defines the lifetime of a particular eddy.

$$T_E = \frac{l}{\sqrt{\frac{2k}{3}}}$$

- **Particle residence (T_R)**:
  Parameter that defines the time in which the particle resides within the eddy.

$$T_R = \frac{l}{|\overline{U} - \overline{U}_p|}$$

- **Interaction time (T_I)**:
  Parameter that defines the actual interaction time between the eddy and the particle. This is simply the minimum of the above defined two time scales.

$$T_I = min(T_R, T_E)$$

- **Fluctuations (U', T')**:
  Parameter that defines the actual value of the fluctuation velocity component. It is obtained by taking a random sample from a normal distribution.

$$U' = \mathcal{N}\left(0, \sqrt{\frac{2k}{3}}\right)$$

  Once the velocity fluctuations are found out, the fluctuations in the temperature field are obtained from the ratio $\frac{U'}{\overline{U}}$ as:

$$\frac{T'}{\overline{T}} = \frac{U'}{\overline{U}}$$

Thus a random sample from the above defined normal distribution gives the velocity fluctuation. This fluctuation is valid only for an interaction time (T_I), after which a new random sample is taken. This is done to mimic the highly unsteady nature of turbulence.

2.2.2 Assumptions for DRW :

- Turbulence is isotropic. This means that the fluctuations are the same in both streamwise and spanwise direction, i.e. $U' = V'$
- When considering multiple particle system, the interaction time for the particles are considered to be constant and equal to the minimum of all the interaction times of the particles
$$T_I = min(T_I^i)$$
- The fluctuations are assumed constant for an interaction time and changes only when the particle position changes, resulting in a new interaction time
- Only one way coupling is assumed. This means that any change in the particle properties will not affect the fluid properties

2.2.3 Material Properties:

Fluid properties such as density (ρ), viscosity (μ), specific heat capacity (C_p), etc are directly obtained from database of RefPropm. It is integrated into MATLAB and the values are used as variables in the code. This is done because the fluid has a varying temperature field in the domain and all these properties are temperature dependent.
The properties of dispersed phase are summarized in the table 2.1.

ρ	1195 kg/m^3
k	0.14 $W/(mK)$
C_p	980 J/kgK
α	1.195 e-7 m^2/s

Table 2.1: Properties of dispersed phase

The particle specification is summarized in the table 2.2

Initial particle diameter	140 μm
Porosity	0.3
Number of particles	100
Initial particle temperature	300 K
Critical moisture content	0.05

Table 2.2: Particle specification

2.3 Drying kinetics

Drying kinetics of the wet particles basically deals with the equations to be used to solve for the drying process. The transport phenomena is explained with the help of a three stage drying model. It comprises of

1. First drying stage
2. Second drying stage
3. Final sensible heating stage

2.3.1 First drying stage

The particle is initially assumed to have a liquid envelope surrounding the solid core of the droplet. The first stage deals with evaporation of this liquid envelope until a critical moisture content is achieved. The important result of this stage is that the droplet diameter, D_p, reduces during the first stage and remains a constant after attaining the critical moisture content, i.e., remains a constant after the end of the first drying stage.

The important assumptions during the modeling of the first drying stage include

- Uniform distribution of droplet temperature
- Density of water vapor in air, $\rho_{v,\infty}$ is 0 (Dry air assumption)

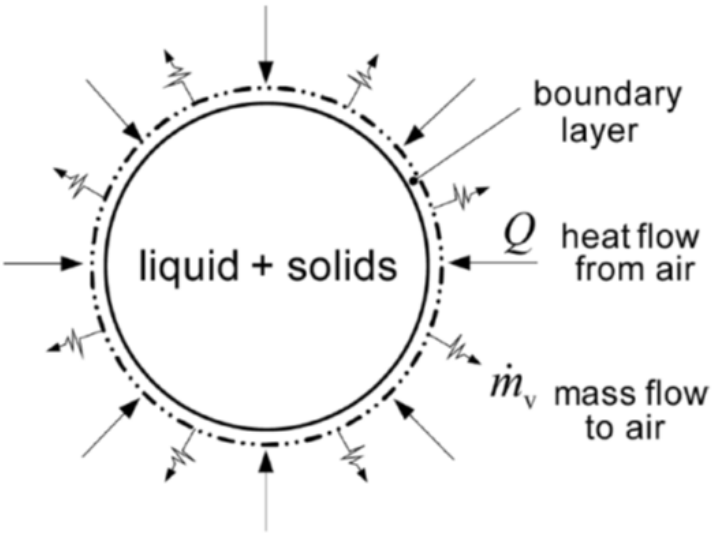

Figure 2.5: First drying stage

The equation of energy conservation is given by

$$h_{f,g}\dot{m}_v + c_{p,d}m_d\frac{dT_d}{dt} = h(T_g - T_d)4\pi R_d^2 \tag{2.1}$$

where,
$h_{f,g}$ - Specific rate of evaporation
$\dot{m}_v$ - Vapor mass transfer rate
m_d - Mass of droplet
T_d - Temperature of droplet
R_d - Radius of droplet
T_g - Temperature of gas

Time rate of change of particle radius is given by the equation

$$\frac{dR_d}{dt} = \frac{-1}{\rho_{d,w} 4\pi R_d^2} \dot{m}_v \tag{2.2}$$

where $\rho_{d,w}$ is the density of water at droplet temperature.

The mass transfer rate from particle surface is determined according to mass convection law,

$$\dot{m}_v = h_D(\rho_{v,s} - \rho_{v,\infty}) 4\pi R_d^2 \tag{2.3}$$

where $\rho_{v,s}$ is the density of vapor on the droplet surface. The first drying stage is completed once the particle attains a critical moisture content of 0.35 [5]. The mass and heat transfer coefficients are calculated using Nusselt and Sherwood number given by :

$$Nu = (2 + 0.6 Re^{1/2} Pr^{1/3})(1 + B)^{-7}$$

$$Sh = (2 + 0.6 Re^{1/2} Sc^{1/3})(1 + B)^{-7}$$

where
Nu - Nusselt number for heat transfer
Sh - Sherwood number for mass transfer
B - Spalding number
Sc - Schmidt number

Particle mass is obtained from

$$m_d = m_{d,o} - \frac{4}{3}\pi \rho_{d,w} [(R_{d,o})^3 - (R_d)^3]$$

where $R_{d,o}$ is the initial radius of the particle.

2.3.2 Second drying stage

In the second drying stage, the particle has a solid core as the external boundary with a wet core inside. The solid core is assumed to be porous and capillaries present in it, through which the liquid core evaporates. This is depicted in figure 2.6.

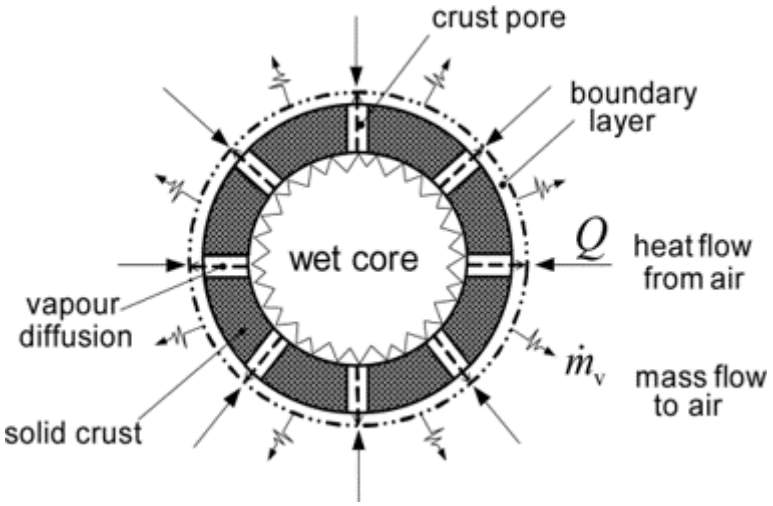

Figure 2.6: Second drying stage

The main assumptions for modeling this stage are:

- Crust thermal conductivity is independent of temperature
- Wet particle has isotropic physical properties
- Crust is pierced by a large number of capillaries

The energy conservation in the crust is given by :

$$\frac{\partial T_{cr}}{\partial t} = \frac{\alpha_{cr}}{r^2}\frac{\partial}{\partial r}(r^2\frac{\partial T_{cr}}{\partial r}), \qquad R_i(t) \leq r \leq R_p$$

where T_{cr} is the temperature of the crust and α_{cr} is the thermal diffusivity of crust.

Energy conservation in the wet core is given by

$$\rho_{wc}c_{p,wc}\frac{\partial T_{wc}}{\partial t} = \frac{1}{r^2}\frac{\partial}{\partial r}(k_{wc}r^2\frac{\partial T_{wc}}{\partial r}), \qquad 0 \leq r \leq R_i(t)$$

The interface receding rate is given by

$$\frac{dR_i}{dt} = \frac{-1}{\epsilon\rho_{wc,w}4\pi R_i^2}\dot{m}_v$$

The boundary conditions for the above equations are;

$$\frac{\partial T_{wc}}{\partial r} = 0, r = 0;$$

$$T_{wc} = T_{cr}, r = R_i(t);$$

$$k_{cr}\frac{\partial T_{cr}}{\partial r} = k_{wc}\frac{\partial T_{wc}}{\partial r} + h_{fg}\frac{\dot{m}_v}{A_i}, r = R_i(t);$$

$$h(T_g - T_{cr}) = k_{cr}\frac{\partial T_{cr}}{\partial r}, r = R_p;$$

where k_{wc} is the thermal conductivity of wet core, k_{cr} is the thermal conductivity of crust and ϵ is the particle crust porosity

The end of the second stage is marked by the moisture content of the droplet dropping to 0.05 [4]. Thus by the end of this stage, maximum water content is removed from the particle.

2.3.3 Sensible heating stage

The particle is now in the form of a non-evaporating dry particle since it has reached the minimal moisture content specified. The almost dry particle is allowed to interact with the hot surrounding air by heat transfer. The heating persists until particle burnout temperature is reached.

The important assumptions for this drying stage include:

- Lumped mass system
- Uniform temperature distribution

The only equation involved in the sensible heating stage is the energy conservation of the final particle given as :

$$c_{p,d} m_p \frac{dT_p}{dt} = h(T_g - T_p) 4\pi R_p^2$$

3 Results and Discussion

The results of the drying kinetics model are discussed in this section. A qualitative comparison of the drying kinetics is given and the result of the computation is validated the three-stage drying kinetics model proposed by Mezhericher [5]. Three main parameters are chosen; the effect of inlet air velocity, the effect of initial moisture content and the effect of inlet air temperature and their effect on the particle size distribution is analysed. An optimum is brought about, in a stepwise manner. For every parametric analysis, the other parameters are kept a constant.

3.1 Qualitative analysis

The drying process is controlled by the rate of moisture diffusion from the particle wet core through the crust pores towards the particle outer surface. As a result of the hindered drying, the particle wet core shrinks and the thickness of the crust region increases. The particle outer diameter is assumed to remain unchanged during the second drying stage. After the point when the particle moisture content decreases to a minimal specified value, the particle is treated as a dry non-evaporating solid sphere. The drying kinetics model implemented is illustrated in figure 3.1a and is compared to the analysis done by Mezhericher 3.1b. A good agreement in the trend of the drying stages is seen as shown below

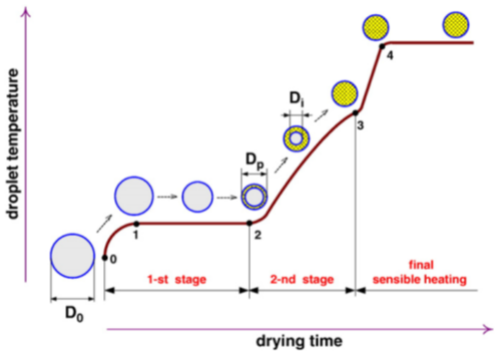

(a) Three-Stage Drying Kinetics as proposed by Mezhericher et al. [5]

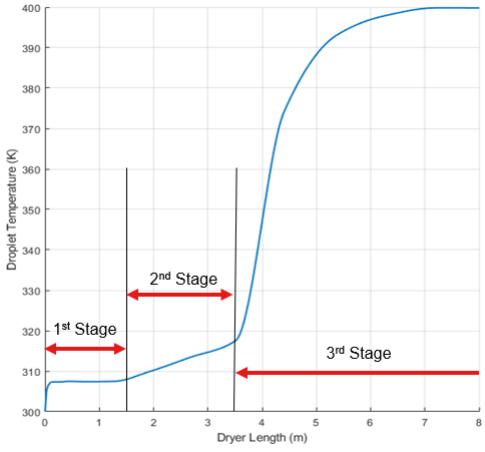

(b) Three-Stage Drying Kinetics obtained from Simulation

Figure 3.1: Qualitative analysis

3.2 Effect of inlet air velocity

Evaporation and particle diameter reduction occur only in the first stage, hence, primary focus is given for the first stage. The effect of inlet air velocity on the drying kinetics is studied. Inlet air flow rate affects only the second stage as seen in the figure 3.2a. The analysis is done with respect to the dryer length. Not much difference in the temperature plots for the first stage is seen. Higher the flow rate, more is the dryer length required to reach the third stage. Another figure 3.2b representing the droplet moisture fraction with drying length for different air velocities is depicted in figure. The critical moisture content is reached at a greater dryer length for the higher inflow velocity and is lower for a lower velocity.

The effect of inlet air velocity on the particle size distribution is depicted in the figure 3.3. A decreased standard deviation in the particle size, meaning a uniform particle size distribution is attained at a velocity of 10 m/s. The lowest standard deviation obtained at $u = 10$ m/s is 0.061 μm. For this analysis, an initial moisture content of 0.4 and an inlet air temperature of 400 K is considered.

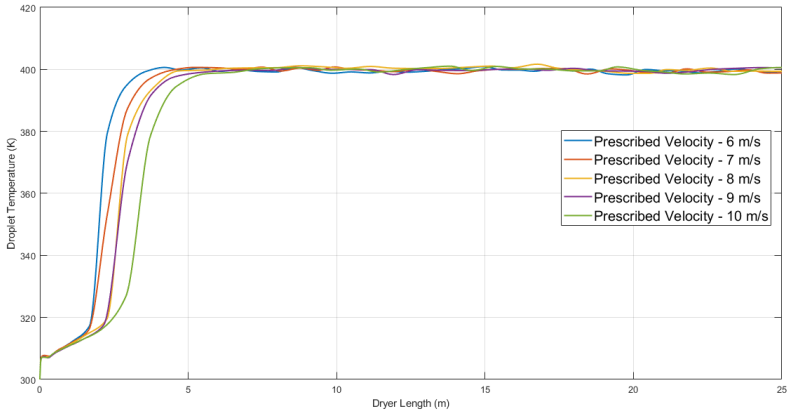

(a) Droplet temperature vs dryer length

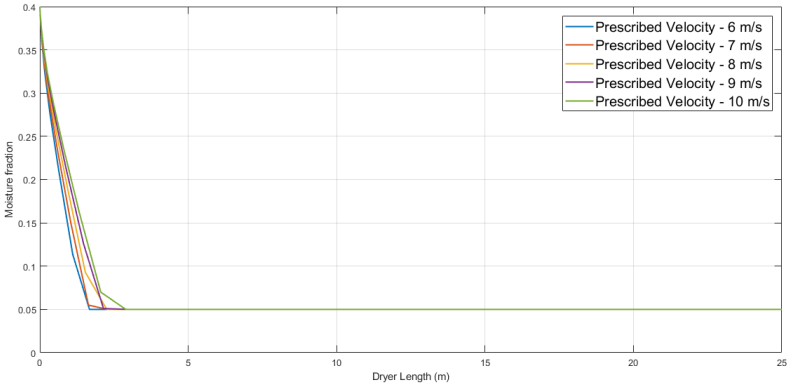

(b) Moisture fraction vs dryer length

Figure 3.2: Effect of inlet air velocity

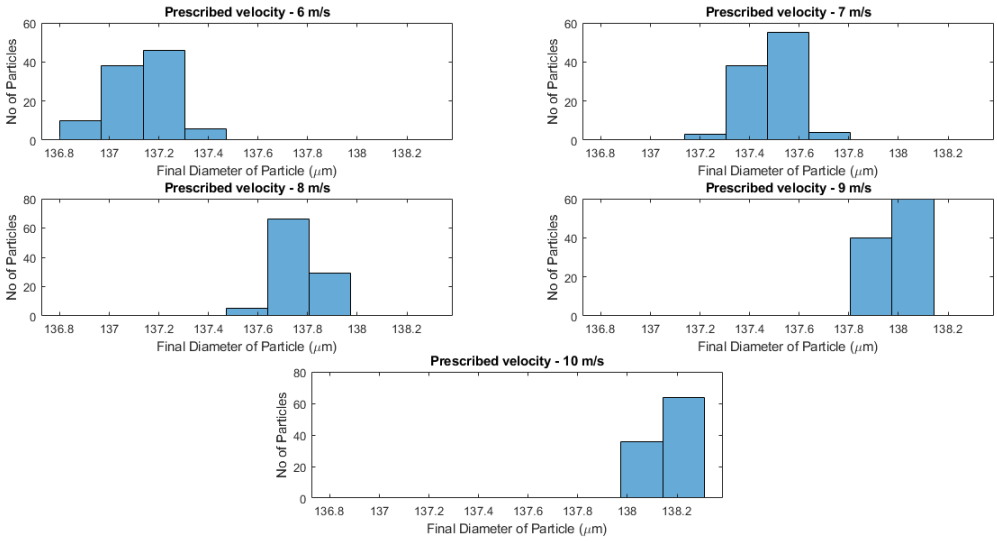

Figure 3.3: Effect of Inlet Air Velocity- Particle Size Distribution

3.3 Effect of initial moisture content

The effect of initial moisture content on the drying kinetics is shown in figure 3.4a. It is observed that the inlet moisture content highly affects the time spent by the particles in the first stage. This in turn corresponds to the increase in dryer length. Higher the inlet moisture content more the time spent in the first stage. The same trend arising from the first stage is seen to continue in the second stage. In another plot 3.4b , the variation of droplet moisture fraction with drying length for different initial moisture contents is shown. The critical moisture content is reached at a greater dryer length for the higher moisture content and at a lower length for a lower moisture content.

The effect of initial moisture content on the particle size distribution is shown in figure 3.5. It is observed that, lesser the moisture content, better is the particle size uniformity. Lesser the time spent in the first stage, better is the particle size uniformity. The lowest standard deviation of 0.065 μm is obtained at an initial moisture content of 0.4 by considering the initial air temperature as 400 K and the air inlet velocity as 10 m/s (optimum condition from previous analysis).

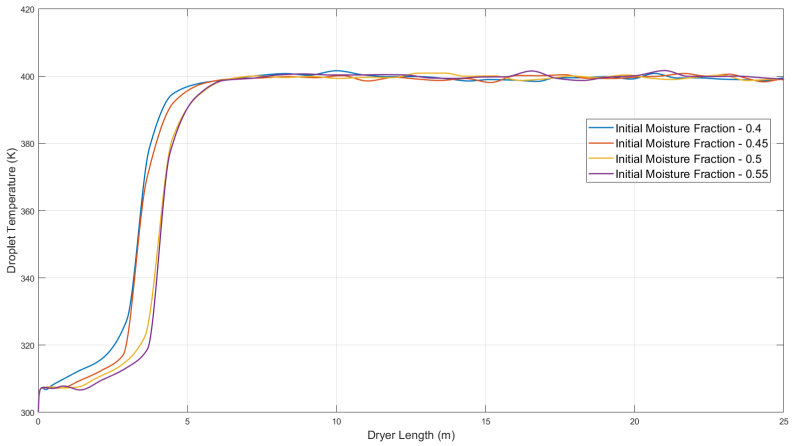

(a) Droplet temperature vs dryer length

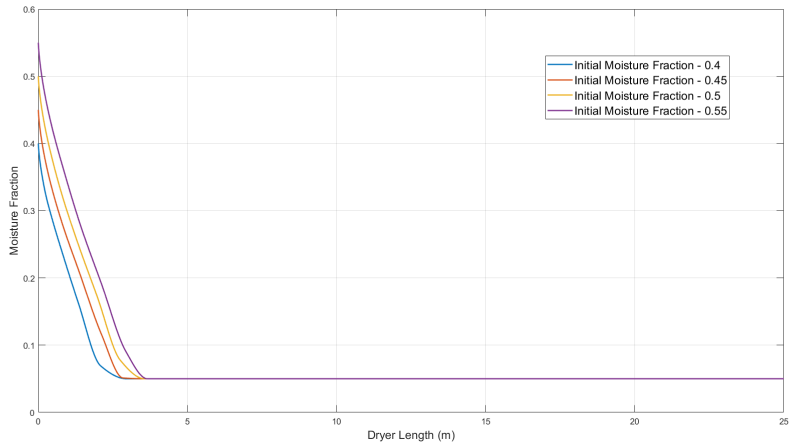

(b) Moisture fraction vs dryer length

Figure 3.4: Effect of inlet air temperature

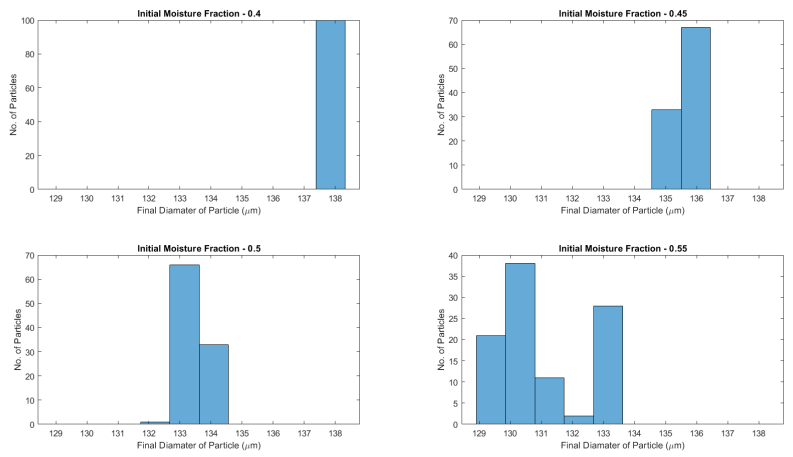

Figure 3.5: Effect of initial moisture content - particle size distribution

3.4 Effect of inlet air temperature

The effect of inlet air temperature on the drying kinetics is shown in figure 3.6a. Inlet air temperature has a significant effect on the first stage as explicitly seen in figure. Higher the temperature, lesser the time spent by the particle in the first stage of the drying kinetics. The trend taken by the particles in the first stage continues into the next two stages. In a secondary plot (figure 3.6b) representing the change in moisture fraction vs dryer length, it is observed that the critical moisture content is reached for the highest temperature faster, and at a lesser drying length than a lower temperature, for which a greater drying length is required.

Finally, the effect of inlet air temperature on the particle size distribution is shown in figure 3.7. It is seen explicitly that, higher the inlet air temperature, better is the particle size uniformity. The lowest standard deviation obtained is 0.052 μm at the optimum conditions obtained from previous analyses, i.e., an inlet air velocity of 10 m/s and an initial moisture content of 0.4.

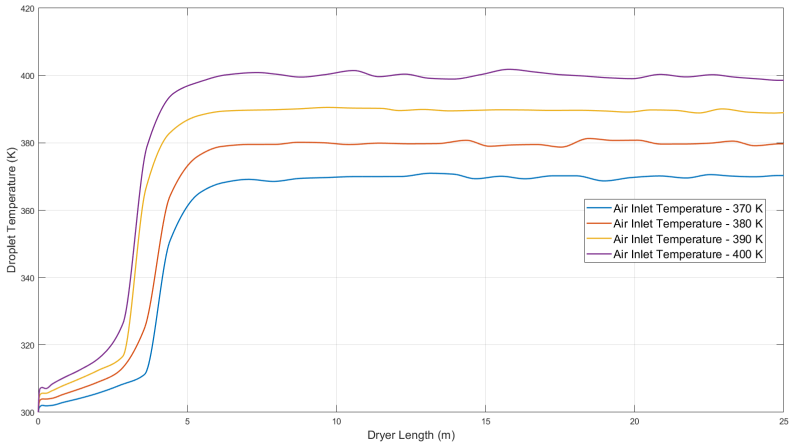

(a) Droplet temperature vs dryer length

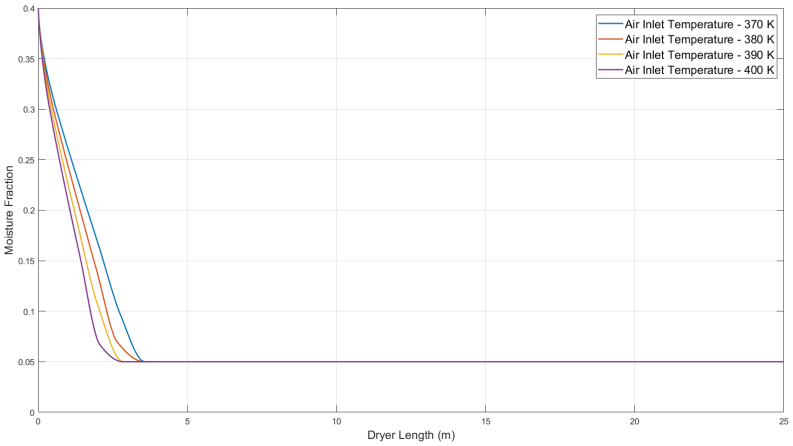

(b) Moisture fraction vs dryer length

Figure 3.6: Effect of inlet air temperature

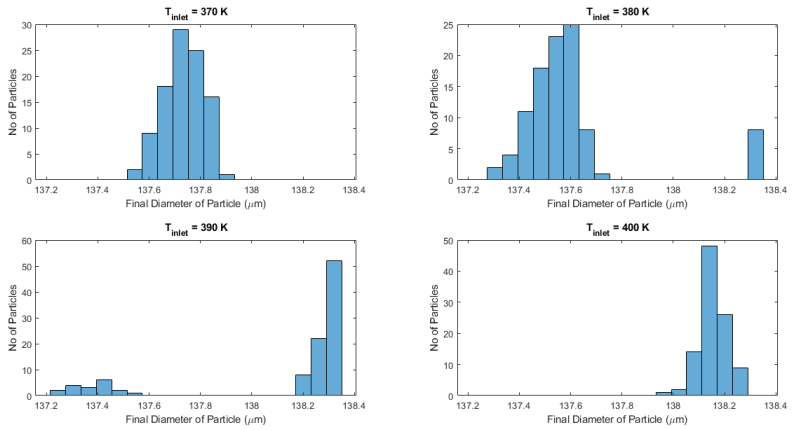

Figure 3.7: Effect of inlet air temperature - particle size distribution

3.5 Sensitivity analysis

Once inlet air velocity, initial moisture content and inlet air temperature is chosen as the primary variables in prescribing the preliminary design for the dryer, it is important to analyze the relative sensitivity of these parameters. Standard deviation of the particle diameter is chosen as the basis on which the sensitivity analysis is done. Effect of inlet air velocity is analyzed first. An initial moisture fraction of 0.4 and an air inlet temperature of 400 K is considered for this analysis (based on the optimum as discussed previously). It is observed (Figure 3.8a) that there is no significant change in the standard deviation for the inlet velocities analyzed. Effect of inlet air temperature is the next chosen parameter for the sensitivity analysis. Air inlet velocity of 10 m/s and an initial moisture content of 0.4 are chosen as constants. It is observed (Figure 3.8b) that there is indeed a significant variation in the standard deviation with change in inlet air temperatures, thereby making this parameter more sensitive than the inlet air velocity.

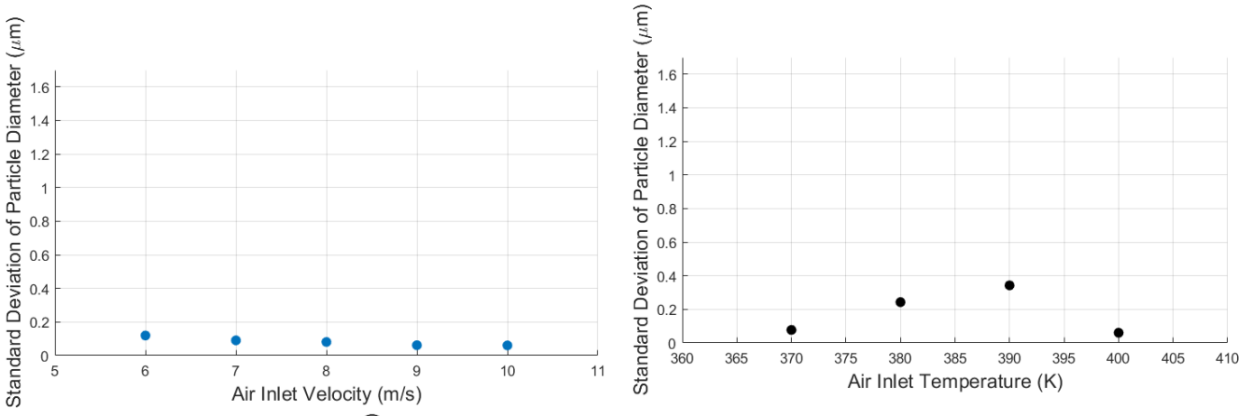

(a) Particle σ vs Dryer length

(b) Particle σ vs Dryer length

Figure 3.8: Sensitivity analysis for air inlet velocity and inlet temperature

Initial moisture content forms the final part of the sensitivity analysis. Air inlet temperature is kept at 400 K and inlet air velocity, at 10 m/s. It is observed (Figure 3.9) that initial moisture content is the most sensitive of the considered parameters, since a huge jump in the standard deviation of particle diameter is observed in the initial moisture range of 0.5 to 0.55. This is not seen in the previous analysis and hence the decreasing order of sensitivity is observed as: initial moisture content, inlet air temperature and air inlet velocity.

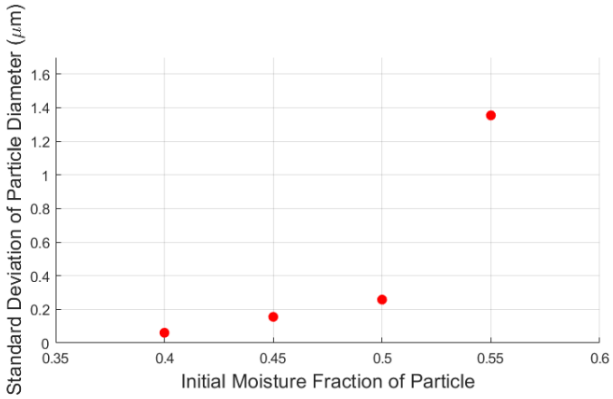

Figure 3.9: Sensitivity analysis for initial moisture content

3.6 Dryer length estimation

Once the parameters required for the particle analyses are understood, it is important to use the available optimum data to obtain the drying length required. Burnout temperature for PVC was assumed to be 380 - 390 K. Analysis of droplet temperature as a function of dryer length is done considering the burnout temperature. Dryer length in the range of 3.5 - 4 m was observed to correspond to the burnout temperature as shown in Figure 3.10a. To validate this dryer length, another analysis was done to extract the particle moisture fraction trend through the three drying stages. It is observed that, a dryer length of 3.5 - 4 m corresponds to a region where the particles have safely reached their critical moisture content (refer figure 3.10b).

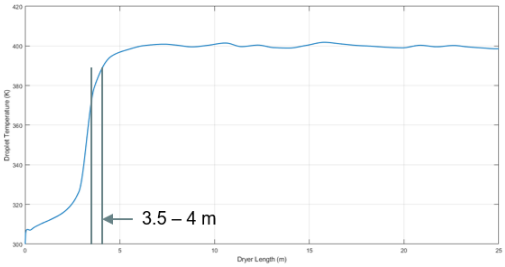

(a) Droplet temperature vs Dryer length

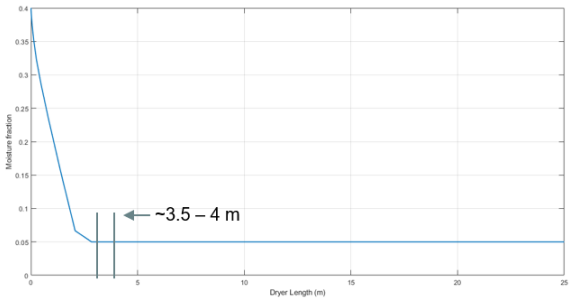

(b) Particle moisture fraction vs dryer length

Figure 3.10: Dryer length analysis

4 Conclusions and Recommendations

The project deals with a preliminary design of a pneumatic dryer. Single phase was solved using a k-ϵ. Once the forces on the particles were obtained, the drying kinetics of the particles was solved. Air inlet velocity, inlet air temperature and initial moisture content were considered as the important parameters for obtaining their optimum operating values. Sensitivity analysis to assess the relative importance of the above-mentioned parameters was performed. Finally an analysis into an optimum drying length was also done and the conclusions drawn are presented as follows:

- Regarding uniformity in particle size distribution, the following conclusions were drawn:
  - **Air Flow rate** : Higher the air flow rate, faster the heat transfer from dry air to the particle. Better uniformity in particle size distribution is observed at 10 m/s
  - **Moisture content**: Lower the initial moisture content of the particle, faster the completion of the first drying stage. Moisture content of 0.4 was observed to have the least standard deviation in particle size distribution
  - **Inlet air temperature**: Increase in the inlet air temperature was found to result in a better uniform particle size distribution. Hence 400 K was observed to have the best uniform particle size distribution
- In the three-stage drying kinetics model proposed by Mezhericher et al., the particle diameter reduces only in the first stage due to evaporation. It was observed that a higher evaporation rate in the first drying stage resulted in a better uniformity in the particle size obtained
- Faster evaporation relies on a higher air flow rate, higher inlet air temperature and a lower initial moisture content of the particle. Hence it is conclusive from the above observation that the values of parameters obtained lead to a better uniformity in the particle size distribution
- From the sensitivity analysis, the following conclusions were drawn:
  - From the sensitivity analysis, it can be concluded that the air velocity magnitude only has negligible effect on the distribution on the size of the particles as observed before
  - While the size distribution does depend on the temperature of the air inlet, the results will be more sensitive to the initial particle moisture fraction as

it increases. Hence, more careful consideration should be given to the initial particle moisture fraction

Based on the above conclusions, the design recommendations are specified as follows:

Recommendations to dry 140 µm PVC particles:

- Dryer length: 3.5 -4 m
- Dryer diameter: 1.25 m
- Inlet air velocity: 10 m/s
- Inlet particle moisture fraction: 0.4
- Inlet air temperature: 390-400 K

Drawbacks and future recommendations:

- Only one way coupling is considered. Multi-way coupling could better model the actual flow phenomena
- 2-D channel is assumed, hence the spanwise turbulence is neglected. A 3-D modeling of the flow phenomena is a more accurate approach and accounts for spanwise turbulence.
- Single phase was assumed to be statistically stationary. Unsteady simulations could better model the forces acting on the particles (history forces, virtual mass effect, etc.)
- Particle agglomeration is not considered.
- Collisions between the particles is neglected. Incorporating collisons could give a clarity on the complicated flow phenomenon in the channel
- DRW model is used to randomize fluctuations. A more physical model could be used to accurately model the effects of turbulence.
- Only selected values for the parameters were taken and tested upon. An optimization problem involving the effect of all parameters would be more practical.
- Burnout temperature of PVC was assumed to be 380-390 K. A practical approach would be to determine the actual burnout temperature by experimenting and using that value for the analysis

Bibliography

[1] DNS database. `http://turbulence.ices.utexas.edu/`.

[2] Luigi A Antonialli and Aristeu Silveira-Neto. Theoretical study of fully developed turbulent flow in a channel, using prandtls mixing length model. *Journal of Applied Mathematics and Physics*, 6(04):677, 2018.

[3] C Crowe, M Sommerfeld, Y Tsuji, and C Crowe. Multiphase flows with droplets and particles crc. *Boca Raton, FL*, 1998.

[4] M Mezhericher, A Levy, and I Borde. Theoretical drying model of single droplets containing insoluble or dissolved solids. *Drying Technology*, 25(6):1025–1032, 2007.

[5] M Mezhericher, A Levy, and I Borde. Three-dimensional modelling of pneumatic drying process. *Powder Technology*, 203(2):371–383, 2010.

[6] Virendra C Patel, Wolfgang Rodi, and Georg Scheuerer. Turbulence models for near-wall and low reynolds number flows-a review. *AIAA journal*, 23(9):1308–1319, 1985.

[7] LM Portela and RVA Oliemans. Possibilities and limitations of computer simulations of industrial turbulent dispersed multiphase flows. *Flow, turbulence and combustion*, 77(1-4):381–403, 2006.

[8] Ludwig Schiller. "U about the resistance of pipes of different cross section and degree of roughness. *ZAMM-Journal of Applied Mathematics and Mechanics*.

[9] M Wegener, N Paul, and M Kraume. Fluid dynamics and mass transfer at single droplets in liquid/liquid systems. *International Journal of Heat and Mass Transfer*, 71:475–495, 2014.